International Forum on Aeroelasticity and Structural Dynamics
IFASD 2019
9-13 June 2019, Savannah, Georgia, USA

MODEL ORDER REDUCTION FOR COUPLED NONLINEAR AEROELASTIC-FLIGHT MECHANICS OF VERY FLEXIBLE AIRCRAFT

Manuel Lanchares[1], Ilya Kolmanovsky[1], Carlos E.S. Cesnik[1], Fabio Vetrano[2]

[1]University of Michigan
Ann Arbor, Michigan USA
mlanchar@umich.edu
ilya@umich.edu
cesnik@umich.edu

[2]Airbus Operations SAS
Toulouse, France
fabio.vetrano@airbus.com

Keywords: Model order reduction, Balanced truncation, Local-bases, Very flexible aircraft, Piecewise-linear model

Abstract: Model order reduction techniques can be employed to reduce the complexity of high-order very flexible aircraft models, allowing their use for control design. In this paper, a technique based on a local-bases approach is introduced to reduce the original nonlinear problem. Firstly, a piecewise-linear surrogate model is obtained through the interpolation of linearized models. Then, the order of the surrogate model is reduced by projecting periodically its dynamics onto an affine subspace. These affine subspaces are computed by balanced truncation of linearized systems of the original model. Sample numerical results on a high-altitude long-endurance aircraft show that the proposed technique generates accurate reduced order models with a reduction of 90% of the dimension of the system.

1 INTRODUCTION

Models of very flexible aircraft can have hundreds or thousands of states. This poses significant challenges for model-based control because the computational cost of using these models is prohibitive. To obtain suitable control-oriented models, a possible solution is to exploit reduced order models (ROMs). For examples of using ROMs in aeroelastic problem, see [1–4].

One of the most successful MOR approaches is the projection-based MOR [5,6], which is based on approximating the state of the system by its projection onto some subspace defined by a reduced order basis (ROB). Different methodologies have been developed to compute the ROB. For instance, proper orthogonal decomposition (POD) [7] is based on projecting the dynamics of the system into a basis formed by relevant modes of the system. These modes are identified by means of the singular value decomposition (SVD) of a snapshot matrix. Another method is the balanced truncation [8] which is popular in linear control design. This technique relies on truncating those states of the system which are less observable and controllable.

When performing MOR of nonlinear models, the computational cost of evaluating the reduced order model may scale with the dimensionality of the full order model thereby negating potential savings in the computation times when using the ROM [9, 10]. The increase of ROM

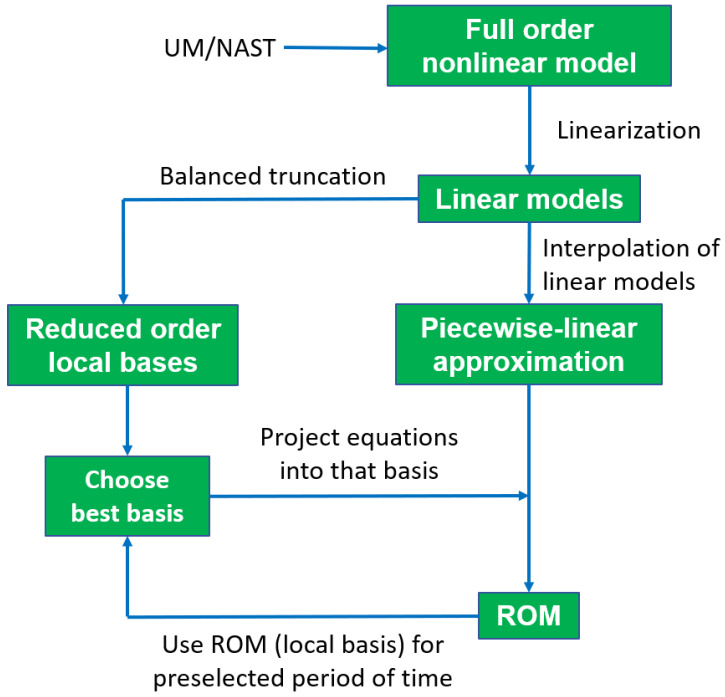

Figure 1: Schematic derivation of a reduced order model based on the reduction of a piecewise-linear model using local-bases obtained by balanced truncation.

complexity can be mitigated by exploiting suitable approximations of the full order model. One of the methods along these lines is based on the piecewise-linear approximation [11, 12]. It is well-known that linear models provide an accurate description of nonlinear models in a neighborhood of the linearization point. Therefore, if linearization points are adequately spaced and an interpolation function is properly defined, then a piecewise-linear surrogate model of the original nonlinear model can be generated through the interpolation of several linear models.

In [11] the piecewise-linear model is reduced using a single global Krylov projection. This approach is not optimal in the sense that a certain projection may be adequate for some region of the state-space but not globally [13]. A possible solution to this is to project the dynamics onto different subspaces (local bases) as the system evolves in time [14]. Most works along these lines in the literature [13–15] treat discrete-time system models and construct the local ROBs based on POD of snapshots grouped into different sets.

In this paper, a ROM of very flexible aircraft is obtained by first constructing the piecewise-linear surrogate model in continuous time and then reducing this model using local bases computed by balanced truncation (see Figure 1). The resulting ROM is a hybrid system with continuous dynamics corresponding to the evolution within each individual ROB and discrete transitions happening when switching between bases. The continuity is preserved in the model output despite switching the bases. The proposed approach is model-based and does not use the snapshots.

The idea of applying balanced truncation to a linear switched system has been explored recently in [16]. However, the system considered in this paper is not a linear switched system of the kind treated in [16], but rather a piecewise-linear model that approximates a nonlinear system. This impedes the direct application of the results in [16] and in [17, 18].

2 PIECEWISE-LINEAR APPROXIMATION

The approach of exploiting piecewise-linear modeling to perform MOR of nonlinear models can be traced back to [11]. The reasons to obtain in the first place a piecewise-linear model from the original nonlinear full order model are as follows:

1. A common problem in MOR of general nonlinear systems is that the computational cost of the ROM scales poorly with the order of the full order model [9, 10, 13] as the reduced order dynamic equations involve the evaluation of high order terms. For a piecewise-linear model, however, this problem can be avoided and the quasi-linear formulation of the problem allows deriving reduced order equations in almost analytical closed form while the interpolation weights are not expensive to compute.
2. In order to perform model order reduction, it is necessary to project the dynamic equations of the system onto some subspace, and these dynamic equations should be in state-space form. This procedure may not be straightforward to apply as the explicit form of the equations may be hidden to the user in certain modeling environments, while piecewise-linear approximation of the model can be generated numerically and circumvents this issue.

A nonlinear model can be approximated by a linear model in the neighborhood of a linearization point, and the nonlinear model can be approximated globally by the interpolation of linearized models. By obtaining N linear models around the points $\mathcal{M} = \{(x^i, u^i),\ i = 1, \cdots N\}$, it is possible to approximate the original nonlinear model of order n with m inputs and p outputs by,

$$\dot{x} = f(x,u) \approx \sum_{i=1}^{N} w_i(x,u)(K_i + A_i x + B_i u), \tag{1}$$

$$y = g(x,u) \approx \sum_{i=1}^{N} w_i(x,u)(L_i + C_i x + D_i u), \tag{2}$$

where the interpolation functions w_i satisfy the conditions,

$$\sum_{i=1}^{i=N} w_i(x,u) = 1, \tag{3}$$

$$w_i(x,u) \geq 0,\ i = 1, \cdots, N, \tag{4}$$

and the matrices K_i, A_i, B_i, C_i, D_i are given by:

$$K_i = f(x^i,u^i) - A_i x^i - B_i u^i, \quad A_i = \left.\frac{\partial f(x,u)}{\partial x}\right|_{(x^i,u^i)}, \quad B_i = \left.\frac{\partial f(x,u)}{\partial u}\right|_{(x^i,u^i)},$$

$$L_i = g(x^i,u^i) - C_i x^i - D_i u^i, \quad C_i = \left.\frac{\partial g(x,u)}{\partial x}\right|_{(x^i,u^i)}, \quad D_i = \left.\frac{\partial g(x,u)}{\partial u}\right|_{(x^i,u^i)}.$$

Clearly, the critical step when constructing the piecewise-linear model is the selection of the set of linearization points $\mathcal{M}$ and of the interpolating functions $w_i(x,u)$. Two approaches are described below to compute these weights.

2.1 Interpolation weights based on distance

Reference [11] defines weights based on the distance,

$$d_i(x,u) = \left\| x - x^i \right\|_2, \tag{5}$$

$$m(x,u) = \min_i d_i(x,u), \tag{6}$$

$$w_i(x,u) = \frac{e^{-\beta d_i(x,u)/m(x,u)}}{\sum_{j=1}^{N} e^{-\beta d_j(x,u)/m(x,u)}}, \tag{7}$$

where β is a weighting parameter to be chosen. Applying this approach to our flexible aircraft models did not provide satisfactory results because the models that were obtained were highly unstable. Therefore, a different approach was pursued with functions $d_i(x,u)$ in Equations (6) and (7) replaced by simpler functions $\zeta_i(x,u)$ that depend on velocity, altitude and Mach number, i.e., typical variables used in aircraft controller gain scheduling. Specific choices used will be discussed later.

2.2 Interpolation weights based on neural network

A more general procedure for constructing the interpolating weights based on neural networks has also been developed.

This procedure exploits a set $S = \{(\dot{x}_k, x_k, u_k)\ k = 1, \cdots, N_s\}$ of the higher fidelity model response where the snapshots contain the values of the state derivative, state, and input values. Next, a function $\xi \colon \mathbb{R}^n \times \mathbb{R}^m \to \mathbb{R}^q$, $z = \xi(x,u)$ that computes a feature vector $z \in \mathbb{R}^q$ is defined. As an example, ξ may be defined as,

$$\xi(x,u) = [V(x), h(x)]^{\mathrm{T}}, \tag{8}$$

where $V(x)$ and $h(x)$ are functions that return the velocity and altitude of the aircraft.

As a result of applying ξ to every linearization point $(x^i, u^i) \in \mathcal{M}$, a set of points $L = \{z_i,\ i = 1, \cdots, N \ \text{ s.t. } \ z_i = \xi(x^i, u^i)\}$ is obtained and their Delaunay triangulation [19] is computed. The purpose of introducing the function $\xi(x,u)$ is to reduce the computational resources needed when performing this triangulation. If there are no restrictions in computational power and enough snapshots are collected, it may be possible to use $\xi(x,u) = [x^{\mathrm{T}}, u^{\mathrm{T}}]^{\mathrm{T}}$.

Next, for each snapshot $(\dot{x}_k, x_k, u_k), k = 1, \cdots, N_s$ the following steps are performed::

1. Set $z_k = \xi(x_k, u_k)$.
2. The points that define the enclosing simplex for z_k of the Delaunay triangulation of L are computed. These points correspond to the linearization points that surround the snapshot $(\dot{x}_k, x_k, u_k)$. For notation purposes, define a set P_k that contains the indeces of these linearization points.
3. All the weights are set to zero except for the ones corresponding to linear models belonging to P_k, which are determined by solving the following optimization problem,

$$\begin{aligned} \min_{w_j^k,\ j\ \in\ P_k} \quad & \|\dot{x}_k - \sum_{j \in P_k} w_j^k (K_j + A_j x_k + B_j u_k)\|^2, \\ \text{s.t.} \quad & \sum_{j \in P_k} w_j^k = 1, \quad w_j^k \geq 0 \text{ for all } j \in P_k. \end{aligned} \tag{9}$$

Finally, a function that returns the weights $w_i(x,u), i = 1, \cdots, N.$ is fit using a feedforward neural network. The neural network is trained based on the inputs $(x_k, u_k), k = 1, \cdots, N_s$ and training targets $w_k, k = 1, \cdots, N_s$.

3 LOCAL-BASES MODEL ORDER REDUCTION

To derive the equations of the ROM, consider the equations that define the projection x_p of a point x onto an affine subspace S_p that passes through an arbitrary point x^0,

$$x_p = x^0 + VP(x - x^0), \tag{10}$$

$$P \triangleq (W^{\mathrm{T}}V)^{-1}W^{\mathrm{T}}, \tag{11}$$

where $x_p, x^0, x \in \mathbb{R}^n$ and $V, W \in \mathbb{R}^{n\times r}$. Note that S_p is defined by the triple (x^0, V, W) and designates an affine subspace of dimension r which passes through x^0 and is parallel to the range of V. The residual of the projection is in the orthogonal complement of the range of W. Rewriting (10), it follows that,

$$x_p = VPx + (I - VP)x^0. \tag{12}$$

Projection-based MOR is based on assuming that the state of the system evolves in a reduced order subspace of the original state-space. In this case, the state of the system is approximated by its projection into S_p. The reduced order state of the system is $x_r \in \mathbb{R}^r$ and is given by,

$$x_r = Px. \tag{13}$$

Substituting Equation (13) into Equation (12) yields the following relationship between the full order state of the system and its reduced order state,

$$x_p = Vx_r + (I - VP)x^0. \tag{14}$$

The dynamics of the ROM corresponding to (1) are,

$$\dot{x}_r = P\dot{x} = Pf(x, u) = Pf(Vx_r + (I - VP)x^0, u), \tag{15}$$

$$y = g(x, u) = g(Vx_r + (I - VP)x^0, u), \tag{16}$$

$$x_r(t = 0) = Px_0, \tag{17}$$

where x_0 is the initial condition in the full order state-space.

Denoting $\delta x = x - x^0$, it is clear from Equation (10) that the quantity that is being approximated is actually δx,

$$\delta x \approx V\delta x_r, \qquad \delta x_r = P\delta x. \tag{18}$$

A linear model in variable δx can be obtained by linearizing the full order nonlinear model around (x^0, u^0). This linear model can be reduced using balanced truncation, obtaining suitable matrices V and W for Equation (18) and thus for Equation (10). The resulting reduced order model is expected to be valid locally, i.e., when (x, u) is near (x^0, u^0).

The local-bases MOR extends the above local approximation procedure by updating the ROM at discrete-time instants t_k, with t_0 being the initial time. The following steps are repeated recursively while using the ROM to simulate the system:

1. Find the closest point (x^c, u^c) in $\mathcal{M}$ (the set of linearization points) with respect to the state-input pair, (x_{t_k}, u_{t_k}), of the system at the current update time instant t_k. A suitable metric for the distance should be defined. Typically, the function $\zeta(x, u)$ introduced in Section 2.1 is an appropriate choice. The full order state x_{t_k} is reconstructed based on $x^-_{r_{t_k}}$ (the reduced order state at time t_k immediately before switching the subspace),

$$x_{t_k} = V_{t_{k-1}} x^-_{r_{t_k}} + (I - V_{t_{k-1}} P_{t_{k-1}}) x_{t_{k-1}}, \tag{19}$$

$$P_{t_{k-1}} = (W^{\mathrm{T}}_{t_{k-1}} V_{t_{k-1}})^{-1} W^{\mathrm{T}}_{t_{k-1}}, \tag{20}$$

where the triple $(x_{t_{k-1}}, V_{t_{k-1}}, W_{t_{k-1}})$ defines the subspace in which the state evolved during the previous time interval $[t_{k-1}, t_k]$. For $t_k = t_0$, there is no previous time interval, and Equation (19) is substituted by the relationship,

$$x_{t_0} = x_0, \tag{21}$$

with x_0 being the initial state of the system.

2. Compute V_{t_k}, W_{t_k} with balanced truncation of the linear system corresponding to (x^c, u^c).
3. The affine subspace onto which dynamics are projected during the time interval $[t_k, t_{k+1}]$ is defined by the triple $(x_{t_k}, V_{t_k}, W_{t_k})$, with x_{t_k} obtained from either Equation (19) or (21). The equations of the reduced order model are obtained by particularizing Equations (15)-(16) for the piecewise-linear model derived in Equations (1)-(2):

$$\dot{x}_r = \sum_{i=1}^{i=N} w_i(V_{t_k} x_r + (I - V_{t_k} P_{t_k}) x_{t_k}, u)(K_{r,i,t_k} + A_{r,i,t_k} x_r + B_{r,i,t_k} u), \tag{22}$$

$$y = \sum_{i=1}^{i=N} w_i(V_{t_k} x_r + (I - V_{t_k} P_{t_k}) x_{t_k}, u)(L_{r,i,t_k} + C_{r,i,t_k} x_r + D_{r,i,t_k} u), \tag{23}$$

with

$$K_{r,i,t_k} = P_{t_k} K_i + P_{t_k} A_i (I - V_{t_k} P_{t_k}) x_{t_k}, \quad A_{r,i,t_k} = P_{t_k} A_i V_{t_k}, \quad B_{r,i,t_k} = P_{t_k} B_i,$$

$$L_{r,i,t_k} = L_i + C_i (I - V_{t_k} P_{t_k}) x_{t_k}, \quad C_{r,i,t_k} = C_i V_{t_k}, \quad D_{r,i,t_k} = D_i,$$

$$P_{t_k} = (W^{\mathrm{T}}_{t_k} V_{t_k})^{-1} W^{\mathrm{T}}_{t_k},$$

The dynamical system defined defined by Equations (22)-(23) is initialized at time $t = t_k$ with the reduced order state corresponding to the projection of x_{t_k} onto the subspace defined by $(x_{t_k}, V_{t_k}, W_{t_k})$:

$$x_r(t = t_k) = P_{t_k} x_{t_k}. \tag{24}$$

Note that $x_r(t = t_k)$ is the reduced order state of the system immediately after switching the projection, hence it is possible to denote $x^+_{r_{t_k}} = P_{t_k} x_{t_k}$.

4. The reduced order model is defined by Equations (22)-(24) and is used over the time interval $[t_k, t_{k+1}]$. Then, at time t_{k+1}, go back to Step 1 to update the projection subspace. Figure 2 shows the schematic behavior of the algorithm.

The resulting reduced order model is a hybrid system with continuous dynamics corresponding to the evolution within each individual reduced order basis, and discrete transitions happening when switching between bases. Note that with this algorithm, the reduced order state instantaneously changes when switching the subspace, i.e. $x^-_{r_{t_k}} \neq x^+_{r_{t_k}}$. However, the reconstructed full

order state of the system x_{t_k} does not change when switching the subspace, as the projection subspace chosen at time instant t_k is forced to contain the reconstructed full order state x_{t_k}. Moreover, the output of the system is not discontinuous when switching the subspace.

Indeed, the output of the system immediately before switching the subspace is,

$$y_{t_k}^- = \sum_{i=1}^{i=N} w_i(V_{t_{k-1}} x_{r_{t_k}}^- + (I - V_{t_{k-1}} P_{t_{k-1}}) x_{t_{k-1}}, u)(L_{r,i,t_{k-1}} + C_{r,i,t_{k-1}} x_{r_{t_k}}^- + D_{r,i,t_{k-1}} u). \quad (25)$$

Substituting $x_{t_k} = V_{t_{k-1}} x_{r_{t_k}}^- + (I - V_{t_{k-1}} P_{t_{k-1}}) x_{t_{k-1}}$ in Equation (25), it is possible to obtain $y_{t_k}^-$ in terms of x_{t_k}:

$$y_{t_k}^- = \sum_{i=1}^{i=N} w_i(x_{t_k}, u)(L_i + C_i x_{t_k} + D_i u). \quad (26)$$

On the other hand, the output of the system immediately after switching the subspace is,

$$y_{t_k}^+ = \sum_{i=1}^{i=N} w_i(V_{t_k} x_{r_{t_k}}^+ + (I - V_{t_k} P_{t_k}) x_{t_k}, u)(L_{r,i,t_k} + C_{r,i,t_k} x_{r_{t_k}}^+ + D_{r,i,t_k} u). \quad (27)$$

Substituting $x_{t_k} = V_{t_k} x_{r_{t_k}}^+ + (I - V_{t_k} P_{t_k}) x_{t_k}$ into Equation (27) tields an expression for $y_{t_k}^+$ in terms of x_{t_k}:

$$y_{t_k}^+ = \sum_{i=1}^{i=N} w_i(x_{t_k}, u)(L_i + C_i x_{t_k} + D_i u). \quad (28)$$

Thus $y_{t_k}^- = y_{t_k}^+$.

Finally, given a set $\mathcal{M}$, many terms in Equations (22)-(23) can be pre-computed offline, except for the term $(I - V_{t_k} P_{t_k}) x_{t_k}$. This term is computed online every time that the projection subspace is switched. The size of the matrices in Equations (22) and (23) is independent of the dimension of the high order model, so the computational cost of their evaluation does not depend on the order of the original model.

Computing the term $w_i(V_{t_k} x_r + (I - V_{t_k} P_{t_k}) x_{t_k}, u)$ involves reconstructing the full order state. Further computational savings could be obtained by freezing the weights w_i during the interval $[t_k, t_{k+1}]$, i.e. replacing $w_i(x, u)$ by $w_i(x_{t_k}, u_{t_k}),\ i = 1, \cdots, N \quad t \in [t_k, t_{k+1}]$. This converts the reduced order model into a switched affine model.

4 VERY FLEXIBLE AIRCRAFT MODEL IN UM/NAST

The University of Michigan Nonlinear Aeroelastic Simulation Toolbox (U/M NAST) has been used to model the nonlinear very flexible aircraft system studied here. UM/NAST is a C++ software package that uses geometrically nonlinear strain-based finite elements for the simulation of aeroelastic aircraft. The development of UM/NAST has started in 1998 with the works of Brown [20] and continued (see e.g., [21] [22]) culminating in the development of the code.

4.1 X-HALE model

Most of numerical results presented in this paper are obtained with the X-HALE RRV-6B vehicle, a testbed to study nonlinear aeroelastic phenomena [23]. The operating velocities of this aircraft lie in the range of 10 to 20 m/s. Its wingspan is 6 m, with an aspect ratio of 30.

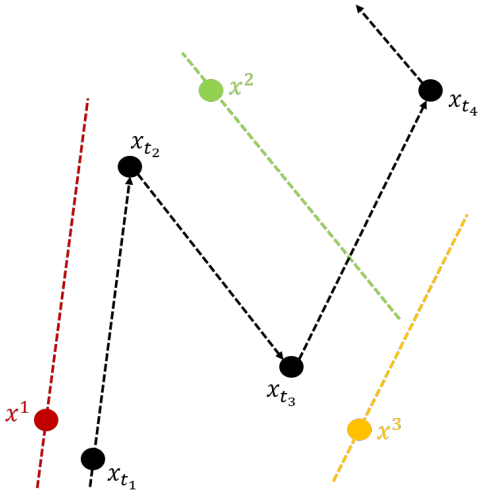

Figure 2: Schematic operation of the local-bases algorithm. The black line represents the trajectory of the state of the system reconstructed from the reduced order state. The colored lines represent affine subspaces obtained by balanced truncation of the linearized models. The projection subspace is switched at time instants t_1, t_2, t_3, t_4. Note that the trajectory of the state of the system belongs to an affine subspace obtained by shifting the affine subspace obtained by balanced truncation of the closest linearized model when the subspace is switched. For instance, at time t_2 the state is x_{t_2}. The closest linearization point is x_2, so the trajectory during the interval $[t_2, t_3]$ belongs to an affine subspace obtained by shifting the green subspace so that it passes through x_2. The green subspace is computed by balanced truncation of the linearized model corresponding to x_2.

The state vector of the very flexible aircraft in UM/NAST is expressed as,

$$x = [\epsilon^{\mathrm{T}} \quad \dot{\epsilon}^{\mathrm{T}} \quad \beta^{\mathrm{T}} \quad \zeta^{\mathrm{T}} \quad P_B^{\mathrm{T}} \quad \lambda^{\mathrm{T}}]^{\mathrm{T}}, \tag{29}$$

where ϵ denotes the elastic states, $\dot{\epsilon}$ denotes their time derivatives, β is a vector of the angular and linear velocities of the aircraft expressed in the body frame, ζ is the quaternion that describes the orientation of the vehicle, P_B is the aircraft center of mass position vector in the inertial frame and λ is the vector of the inflow states. The model has 345 states.

Since model order reduction approximates the input-output behavior of the full order model, the outcome is dependent on the selection of inputs and outputs. For the analysis in this report the outputs of primary interest for maneuver load alleviation have been selected so that

$$y = [k_{y,l} \quad k_{y,r} \quad \beta^{\mathrm{T}} \quad \zeta^{\mathrm{T}}]^{\mathrm{T}}, \tag{30}$$

where $k_{y,l}$ and $k_{y,r}$ denote the out of plane bending of the left and right wing root, respectively.

Regarding the inputs, the original X-HALE model has 37 inputs. Of these 37 inputs, 2 correspond to the spoilers, 30 to the elevator surfaces, and 5 to the propellers. For the sake of simplicity, in this study the number of inputs is reduced to 5. This reduction is effected by constraining all the elevators to be deflected equally and the propellers to act anti-symmetrically. Therefore, the effective reduced input vector will be:

$$u = [sp_l \quad sp_r \quad e \quad P_0 \quad \delta P]^{\mathrm{T}}, \tag{31}$$

where sp_l and sp_r are the deflections of the left and right spoilers, respectively, e is the deflection of the elevators, P_0 is the thrust of the central propeller, and δP is the differential thrust.

4.2 XRF1 model

The X-HALE model considered here has 345 states. Another model has been employed to show the applicability of proposed model order reduction technique to higher order dimensional models. In particular, the XRF1 aircraft model is used. The XRF1 model is an Airbus provided research testcase to showcase the application of different technologies to a long range wide body aircraft.

This model should be classified as a flexible aircraft model rather than very flexible due to its standard aspect ratio. However, it is significantly more complex than X-HALE as the XRF1 model has 1013 states. Regarding the control effectors, the XRF1 model has nine: two engines to produce thrust, two ailerons per wing, one elevator divided into a right and a left section, and a rudder. In this study, the inner and outer ailerons of each wing are equally deflected, so the effective number of inputs is seven. The output considered for model order reduction is the same of Equation (30).

Figure 3: Plot of XRF1 model aircraft.

5 NUMERICAL RESULTS

The numerical results presented in this section apply mostly to the X-HALE model presented previously. In this sense, subsections 5.1, 5.2, and 5.3 concern the X-HALE model, whereas subsection 5.4 deals with the XRF1 model.

5.1 Linearization of UM/NAST X-HALE model

In general, it is not necessary that the same set of linear models is used in both the piecewise-linear approximation and in the generation of the reduced order basis. For simplicity, in this paper the same set of linear models is used for both purposes. The linear models correspond to trim conditions for altitude 30 meters and velocities $13, 13.25$,...19.75 and 20 m/s, yielding a total of 29 linear models.

The methodology proposed to perform model order reduction relies heavily on the accuracy of the linearizations of the original nonlinear system, as linear models are used in the generation of both the piecewise-linear model and the reduced order bases. Therefore, it is necessary to check how each of the linear models used matches with UM/NAST.

To do so, for every linear model small inputs are applied in each input channel. The time response match between UM/NAST and the linear model is compared. Analyzing the results, it is apparent that the linearized models match well the nonlinear solution in the immediate neighborhood they were generated. For instance, Figure 4 shows the match between UM/NAST and the linearized model for 14 m/s. In this maneuver, the aircraft is flying trimmed at 14 m/s. Then, an elevator doublet of amplitude 1 deg with respect to the trim condition of 14 m/s is applied.

The maneuver shown in Figure 4 excites fundamentally longitudinal dynamics of the system. The mismatch in the lateral velocity, roll rate, and yaw rate output channels - that is, the lateral dynamics outputs - is due to small nonlinear coupling effects between the longitudinal inputs and the lateral outputs. This is highlighted in Figure 5, where the roll rate for different magnitudes of the doublet elevator is shown. It is clear that the linear model matches the nonlinear solution up to a certain point, when nonlinear effects not captured by the linear model start to predominate in the response. As the magnitude of the doublet increases, i.e. as the input moves away from the linearized condition, the nonlinear effects act faster.

Similarly, it has been observed nonlinear coupling effects between lateral inputs and longitudinal outputs. Nevertheless, the magnitude of these nonlinear effects is small and thus do not affect the overall quality of the linear models when approximating the UM/NAST model.

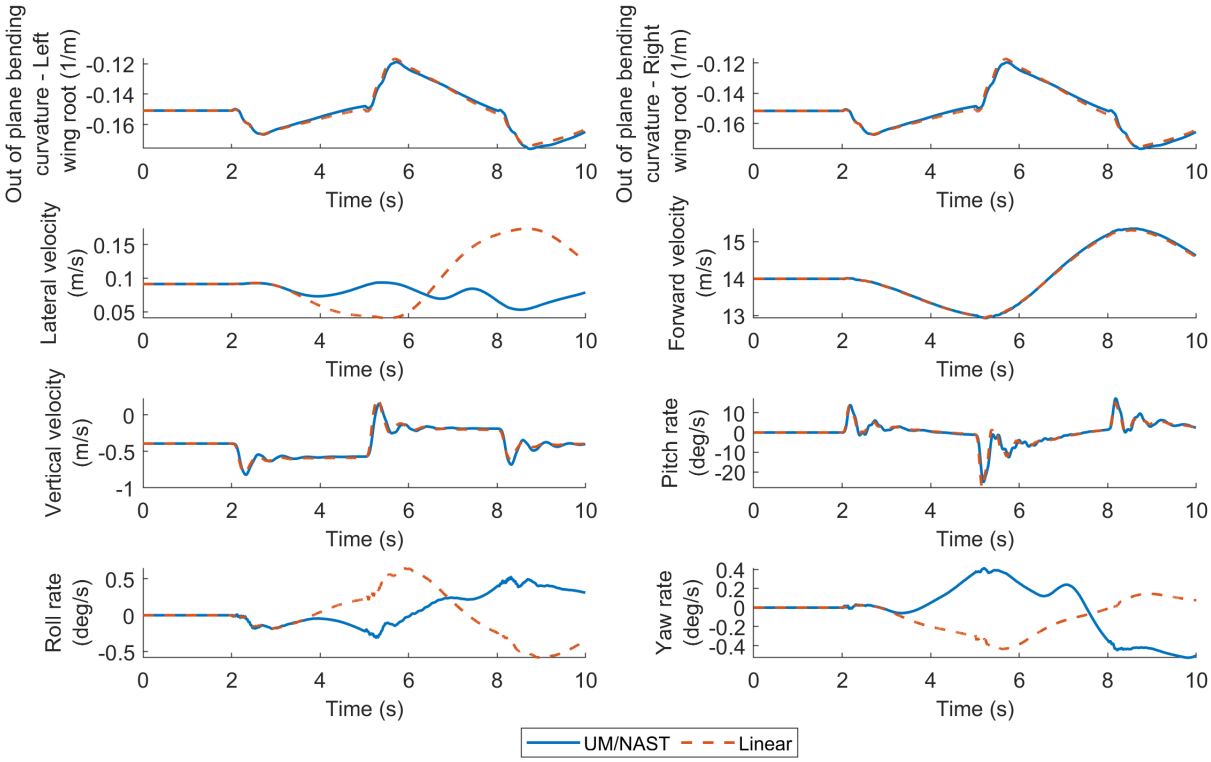

Figure 4: Time response to an elevator doublet maneuver of 1 deg amplitude applied to the X-HALE model initially flying trimmed at 14 m/s. Solid blue line: UM/NAST model. Dashed red line: linear model corresponding to velocity of 14 m/s.

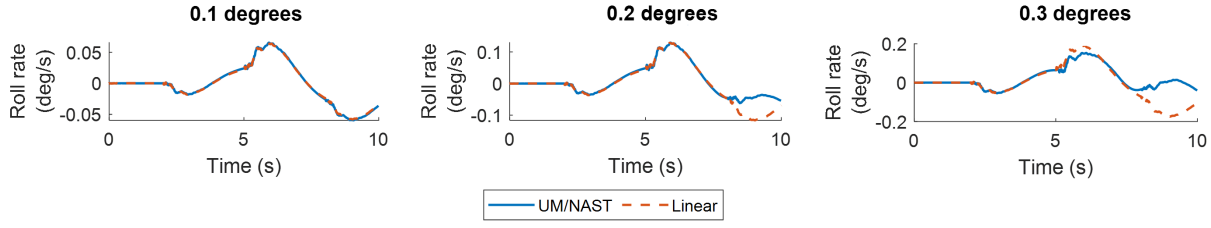

Figure 5: Roll rate response to an elevator doublet maneuver of $0.1, 0.2$ and 0.3 deg amplitudes applied to the X-HALE model initially flying trimmed at 14 m/s. Solid blue line: UM/NAST model. Dashed red line: linear model corresponding to velocity of 14 m/s.

5.2 Piecewise-linear approximation of X-HALE model

In the previous section, it has been discussed that individual linear models capture the dynamics of the nonlinear system in the neighborhood of the linearization point. Hence, these models can be used to create a piecewise-linear model. The main advantage of the piecewise-linear model over any individual linear model is that the piecewise-linear model is accurate across the whole envelope of flight conditions considered, while the linear models are only valid near their linearization point. The two interpolation schemes introduced in subsections 2.1 and 2.2 are evaluated next.

5.2.1 Interpolation weights based on physical insight of the system

For the X-Hale aircraft,functions $d_i(x,u)$ in Equations (6) and (7) are replaced by simpler functions $\zeta_i(x,u)$ that depend on velocity, $\zeta_i(x,u) = \|V(x) - V^i\|_2, i = 1, \cdots, N$, where $V(x)$ denotes the velocity of the aircraft and V^i is the trim velocity of the i^{th} linear model.

The parameter β in Equation (7) is set to 20, which makes the interpolation functions of Equation (7) assign almost all of the weight to a particular linear model. This model is referred as the dominant model at a particular instant of time. Moreover, the transition time when switching from one dominant linear model to the next one is typically small due to the value assigned to β. This characteristic makes the piecewise-linear model behave similarly to a switched system.

The match between UM/NAST, the piecewise-linear model, and a single linear model has been evaluated for several test cases. The individual linear model chosen is the one corresponding to 15 m/s, as 15 m/s is the velocity that lies in the middle of the aircraft velocity range. The results show that the piecewise-linear model consistently achieves a closer match with respect to UM/NAST than the 15 m/s linear model.

One example of such a test case is shown in Figure 6, where a thrust doublet of magnitude 300 RPM is applied to an aircraft flying trimmed at 14 m/s. The small mismatch in the lateral output channels is due to the nonlinear coupling effects decribed above. As these phenomena are not captured by the linear models, the piecewise-linear model does not reflect them too. Finally, note that as the dominant model is switched, no instabilities appear in the piecewise-linear model.

5.2.2 Interpolation weights based on neural network

The function $\xi(x,u)$ was chosen as $\xi(x,u) = V(x)$, where $V(x)$ is the velocity of the aircraft. The neural network architecture is a feedforward neural network with 2 hidden layers and 10 neurons per layer.

Simulations have been performed to compare the performance of the piecewise-linear model using weights based on distance in Section 2.1, and using neural network based weights. Figure 7 compares the responses to an elevator doublet input of 2 deg of amplitude applied to an X-HALE aircraft initially flying trimmed at 14 m/s. The results of Figure 7 along with several other tests conducted for the X-HALE model show that both algorithms achieve similar results.

However, the neural network weighting functions may yield unstable piecewise-linear systems if the set of the snapshots is not sufficiently rich. Another disadvantage of the neural network based weights is that their evaluation is more expensive than the evaluation of the distance-based weights. In the remainder of the paper the distance-based interpolation weights are used.

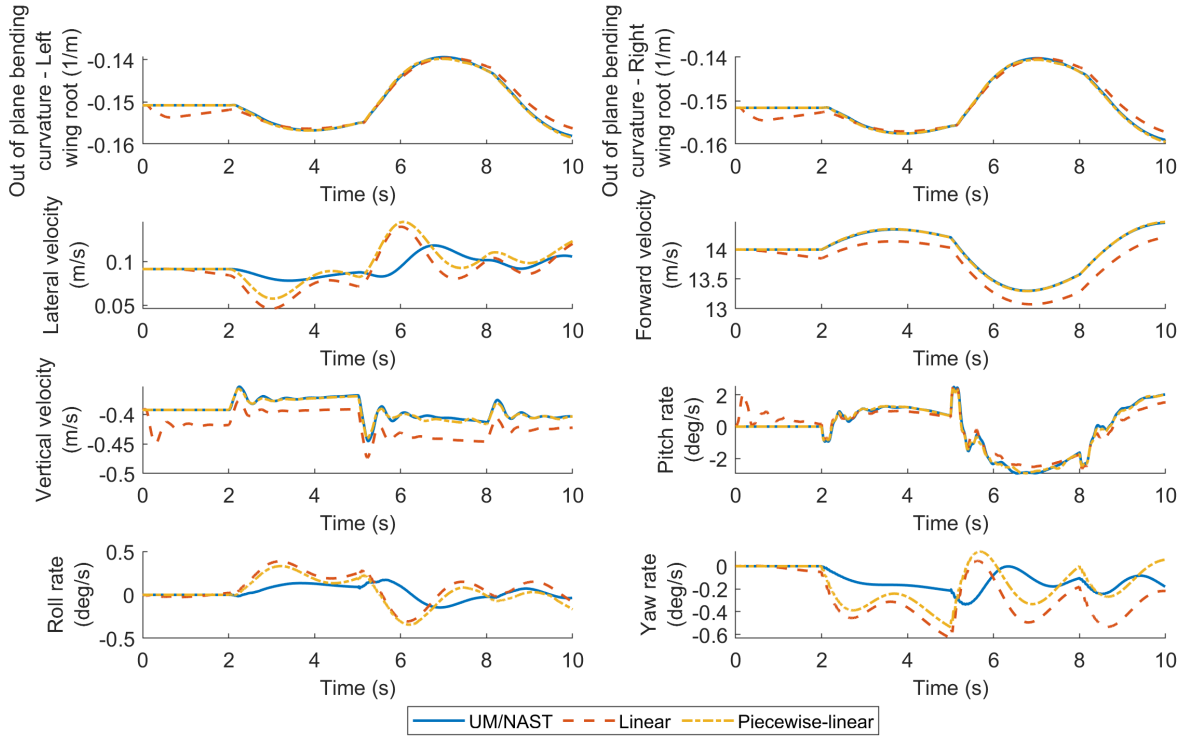

Figure 6: Time response to a thrust doublet maneuver of 300 RPM amplitude applied to the X-HALE model initially flying trimmed at 14 m/s. Solid blue line: UM/NAST model. Dashed red line: linear model corresponding to velocity of 15 m/s. Dashed dotted yellow line: piecewise-linear model with distance-based interpolating weights.

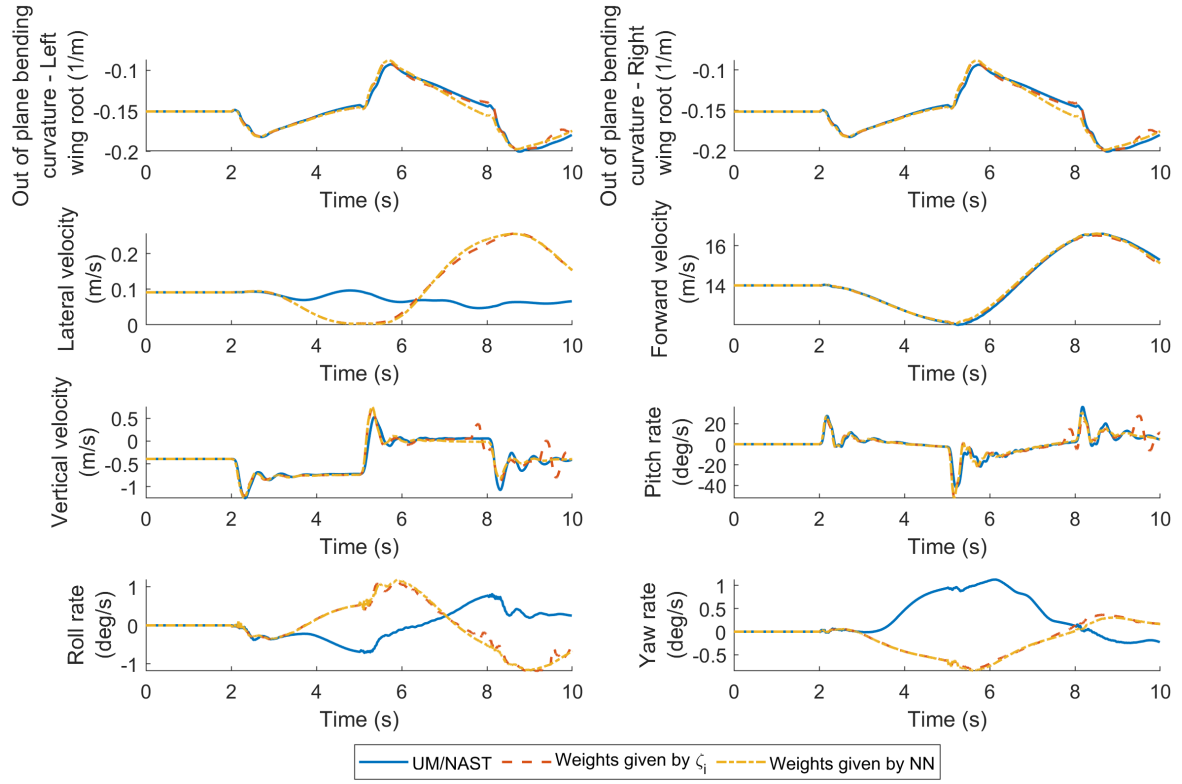

Figure 7: Time response to an elevator doublet maneuver of 2 deg amplitude applied to the X-HALE model initially flying trimmed at 14 m/s. Solid blue line: UM/NAST model. Dashed red line: piecewise-linear model with distance-based interpolating weights. Dashed dotted yellow line: piecewise-linear model with neural network based weights.

5.3 Reduced order model using local bases of X-HALE model

As the next step, the piecewise-linear ROM (22)-(23) has been generated. The local basis used to project the dynamics of the system is chosen to be updated every 0.5 seconds. An important issue is the choice of the dimension of the ROM. Note that the proposed method does not require the reduced order bases to have the same dimension, i.e. the matrices V_{t_k} and P_{t_k} may have different size depending on the basis considered. For simplicity, in the following analysis it assumed that all reduced order bases have the same dimension. The local-bases are obtained through balanced truncation, which also provides an estimate of the error based on the retained energy of the system, measured by the Hankel Singular Values of the associated linear system. Figure 8 shows the Hankel Singular Values of the full order linear model corresponding to 14 m/s. The Hankel Singular Values of the other linear models follow a similar distribution to the one in Figure 8. Most of the energy of the system is captured within 30 states, so this size is an appropriate starting point to choose the dimension of the ROM.

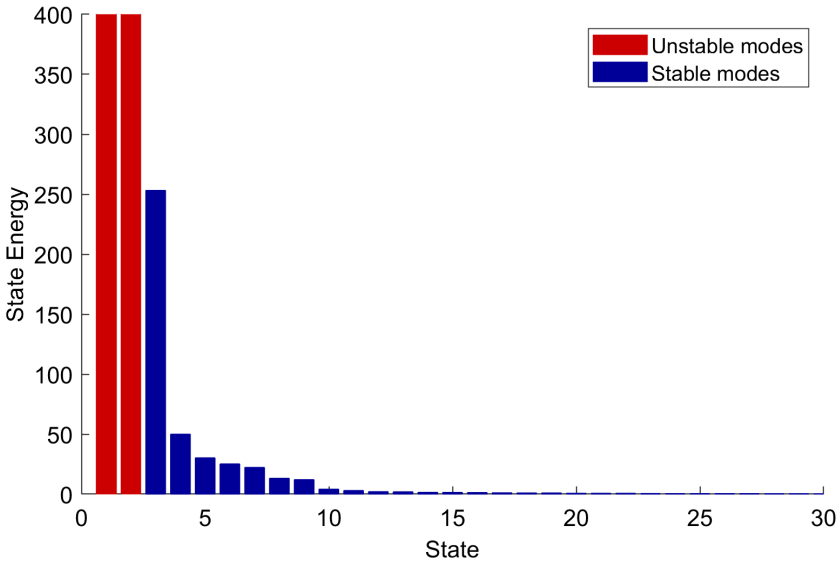

Figure 8: Hankel singular values of the linear model corresponding to 14 m/s.

In order to compare the performance of the method described in this paper, a reduced order model of size 30 has been obtained through balanced truncation of the linear model corresponding to 15 m/s. The time response of UM/NAST, the reduced order piecewise-linear model, and the reduced order linear model is plotted in Figures 9 - 12. Analyzing these figures it is evident that the reduced order piecewise-linear model achieves superior results when compared to the reduced order linear model.

The sensitivity of the accuracy of the reduced order model with respect to its dimension has been evaluated. The root mean square error (RMSE) of the reduced order piecewise-linear model with respect to the UM/NAST solution is computed as function of the dimension of the reduced order model. The results shown in Figures 13 - 16 suggest that using a reduced order model of size bigger than 40 does not yield substantially better accuracy. Note that the error does not reach 0 as the the order increases. This is because there exists a residual error between UM/NAST and the full order piecewise-linear model due to nonlinear effects not captured by the linear models.

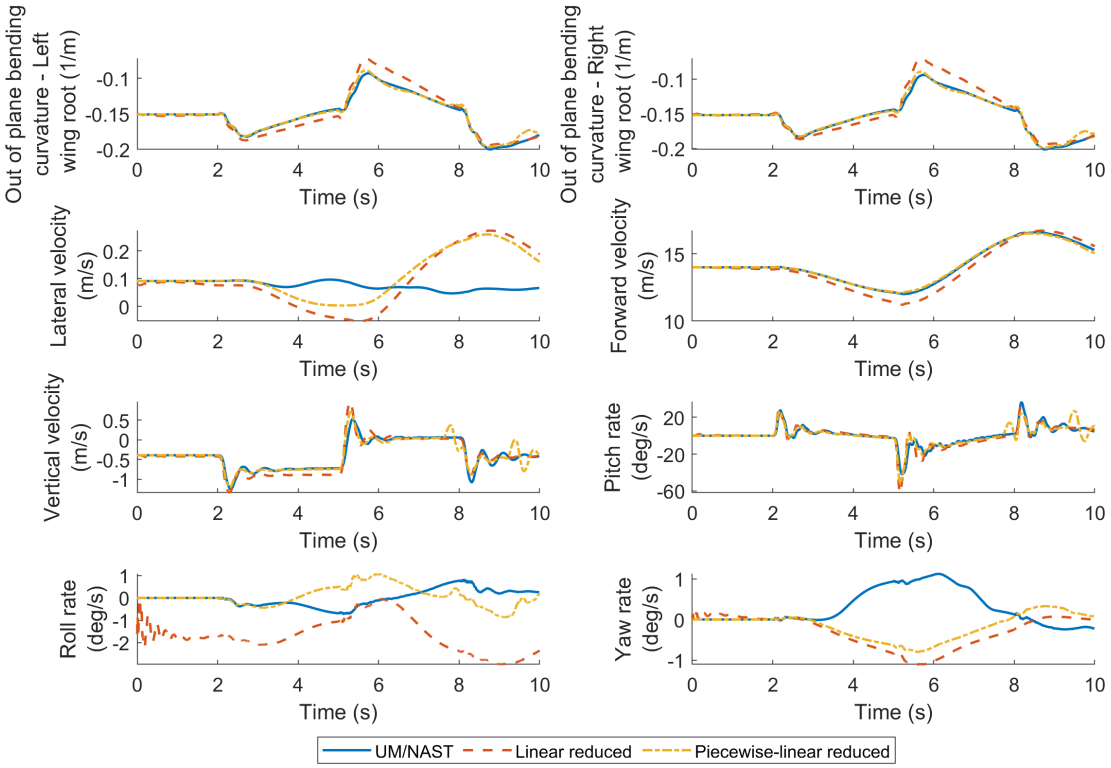

Figure 9: Time response to an elevator doublet maneuver of amplitude 2 deg applied to the X-HALE model initially flying trimmed at 14 m/s. Solid blue line: UM/NAST model (345 states). Dashed red line: reduced order linear model (30 states) corresponding to velocity of 15 m/s. Dashed dotted yellow line: reduced order piecewise-linear model with distance-based interpolation weights (30 states).

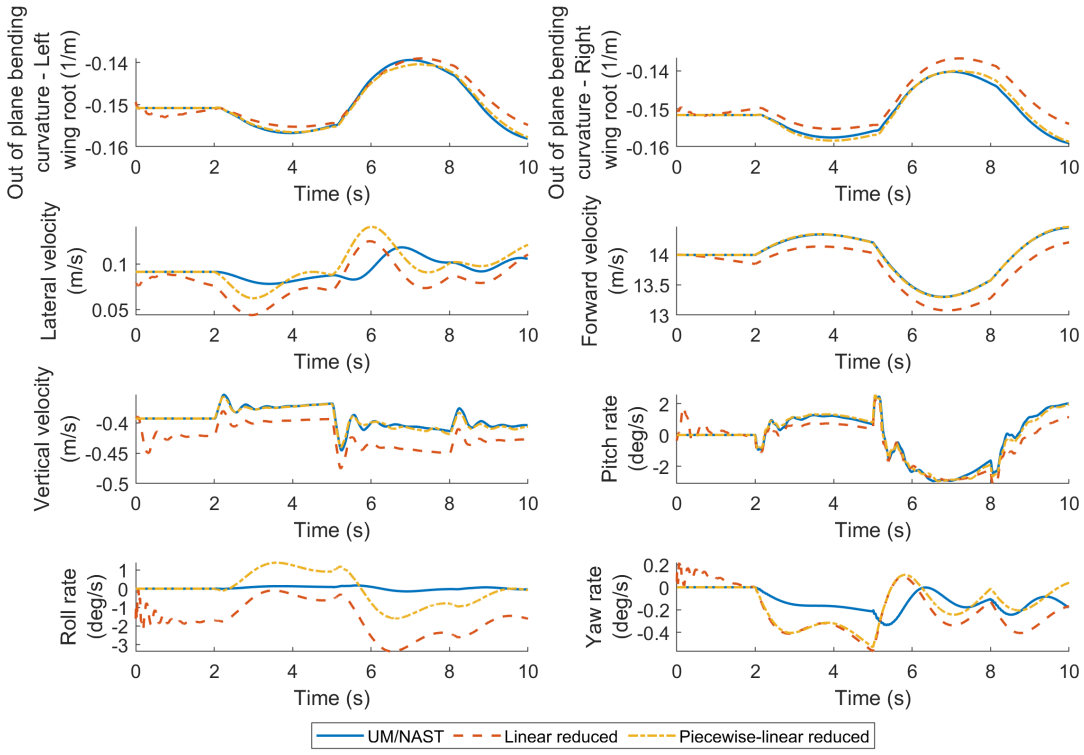

Figure 10: Time response to a thrust doublet maneuver of 300 RPM amplitude applied to the X-HALE model initially flying trimmed at 14 m/s. Solid blue line: UM/NAST model (345 states). Dashed red line: reduced order linear model (30 states) corresponding to velocity of 15 m/s. Dashed dotted yellow line: reduced order piecewise-linear model with distance-based interpolation weights (30 states).

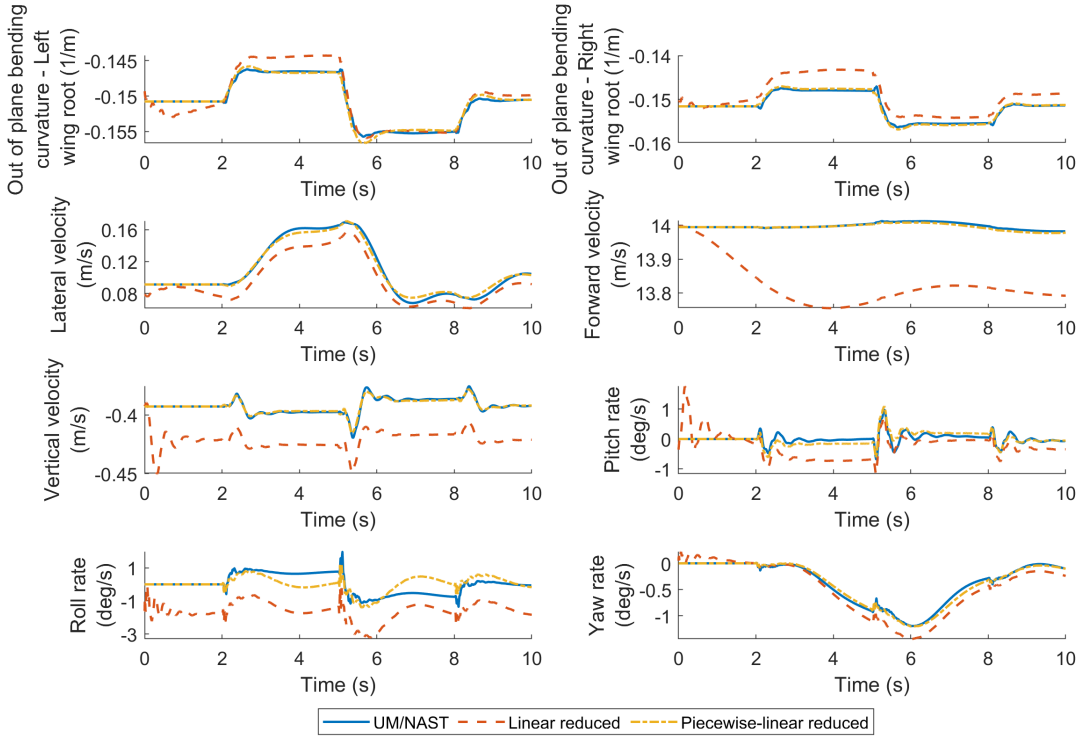

Figure 11: Time response to an aileron doublet maneuver of 2 deg amplitude applied to the X-HALE model initially flying trimmed at 14 m/s. Solid blue line: UM/NAST model (345 states). Dashed red line: reduced order linear model (30 states) corresponding to velocity of 15 m/s. Dashed dotted yellow line: reduced order piecewise-linear model with distance-based interpolation weights (30 states).

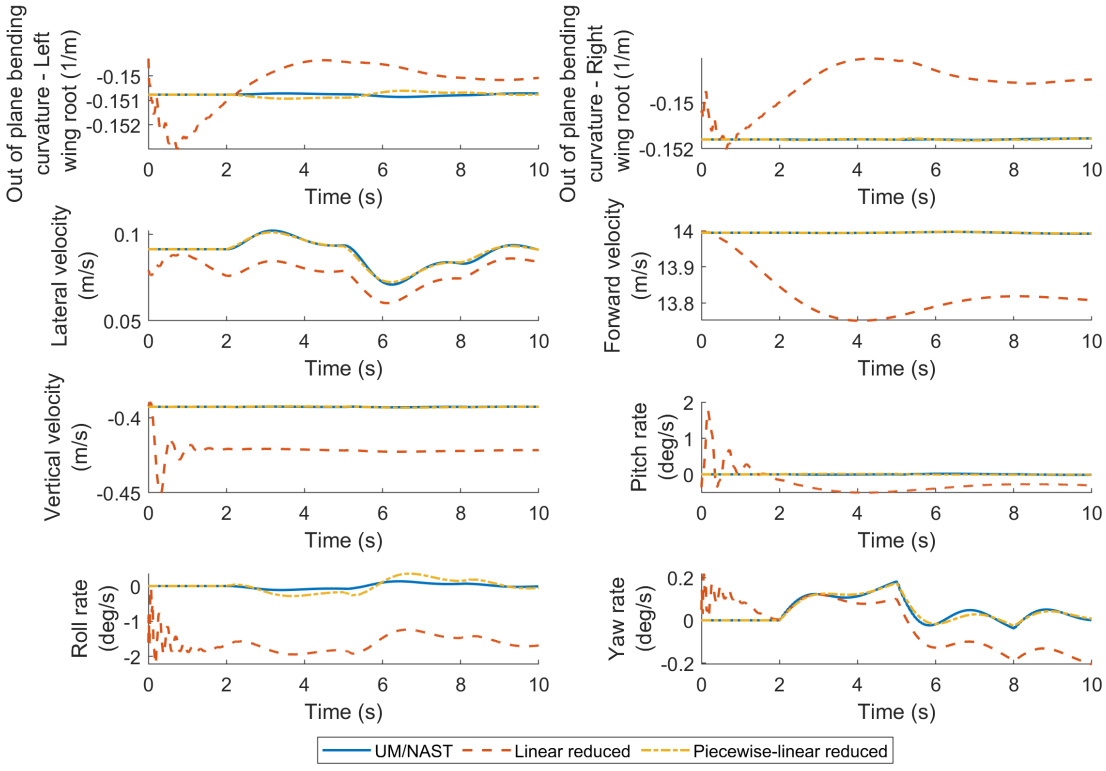

Figure 12: Time response to a differential thrust doublet maneuver of 6 RPM amplitude applied to the X-HALE model initially flying trimmed at 14 m/s. Solid blue line: UM/NAST model (345 states). Dashed red line: reduced order linear model (30 states) corresponding to velocity of 15 m/s. Dashed dotted yellow line: reduced order piecewise-linear model with distance-based interpolation weights (30 states).

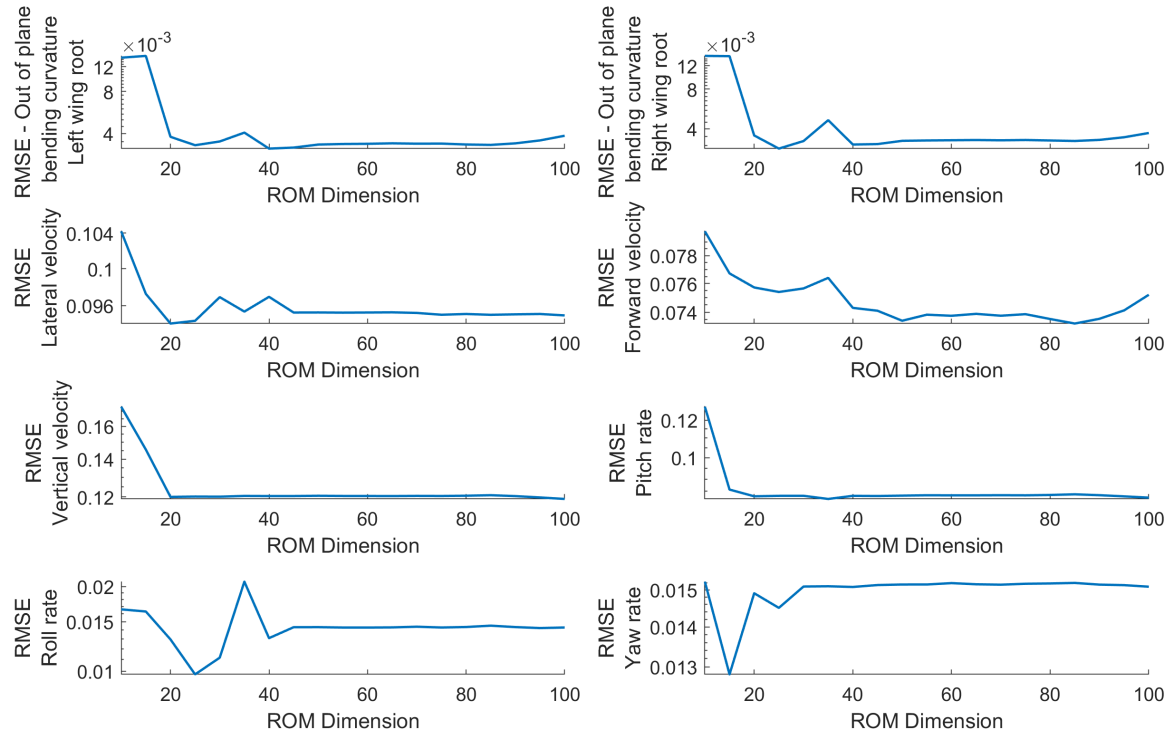

Figure 13: Root Mean Squared Error (RMSE) of the reduced order piecewise-linear model with distance-based interpolation weights with respect to UM/NAST as function of the order of the ROM. The maneuver is an elevator doublet of 2 deg amplitude applied to the X-HALE model initially flying trimmed at 14 m/s.

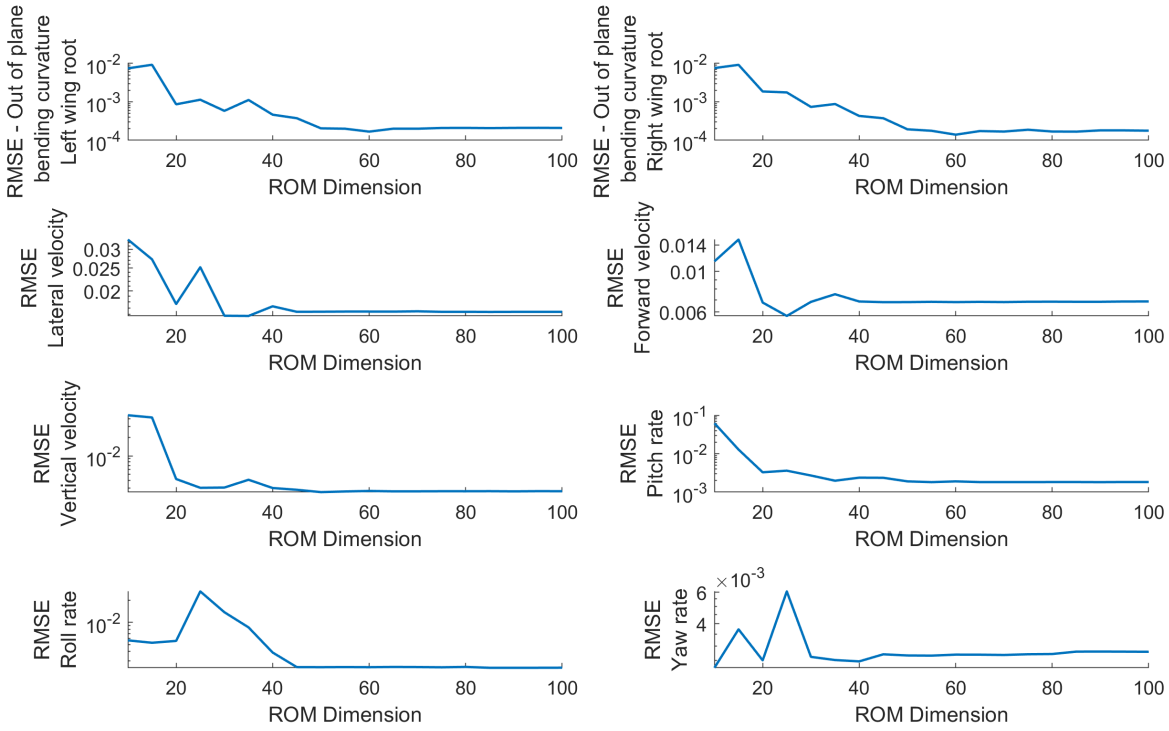

Figure 14: Root Mean Squared Error (RMSE) of the reduced order piecewise-linear model with distance-based interpolation weights with respect to UM/NAST as function of the order of the ROM. The maneuver is a thrust doublet maneuver of 300 RPM amplitude applied to the X-HALE model initially flying trimmed at 14 m/s.

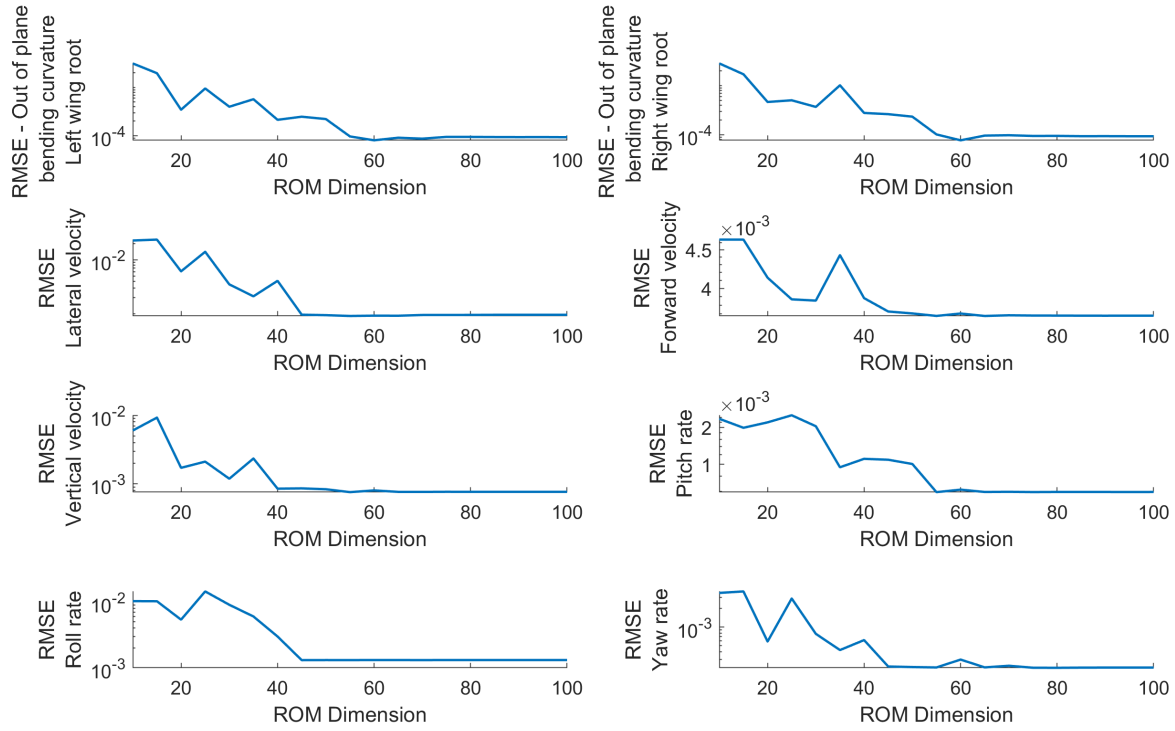

Figure 15: Root Mean Squared Error (RMSE) of the reduced order piecewise-linear model with distance-based interpolation weights with respect to UM/NAST as function of the order of the ROM. The maneuver is an aileron doublet maneuver of 2 deg amplitude applied to the X-HALE model initially flying trimmed at 14 m/s.

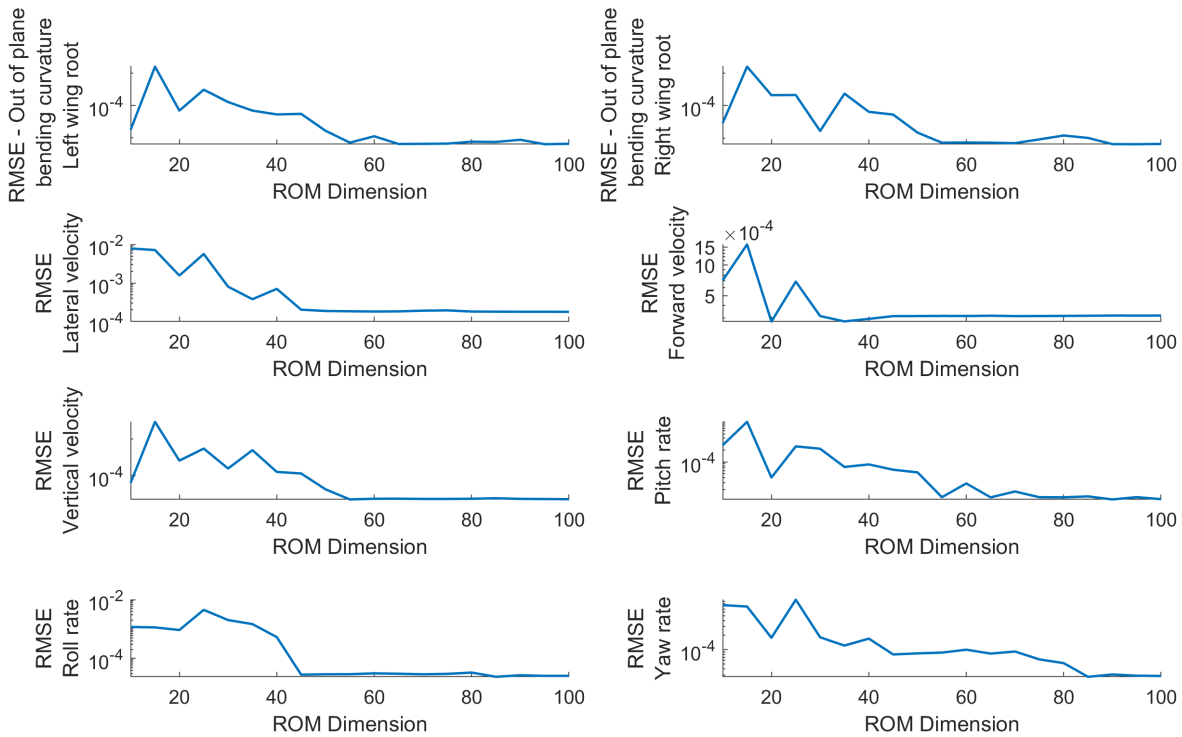

Figure 16: Root Mean Squared Error (RMSE) of the reduced order piecewise-linear model with distance-based interpolation weights with respect to UM/NAST as function of the order of the ROM. The maneuver is a differential thrust doublet maneuver of 6 RPM amplitude applied to the X-HALE model initially flying trimmed at 14 m/s.

5.4 Numerical results for XRF1 model

The XRF1 model is linearized around three altitudes and Mach numbers in transonic range in increments of 0.01. The full order piecewise linear model is generated with $\beta = 20$, and the functions $\zeta_i(x, u)$ are defined as,

$$\zeta_i(x,u) = \left\| \left(\frac{M(x) - M^i}{M^\star}, \frac{h(x) - h^i}{h^\star} \right)^{\mathrm{T}} \right\|_2, \tag{32}$$

where M is the Mach number of the aircraft, and h denotes its altitude in meters. The scaling parameters $M^\star$ and $h^\star$ are chosen to be 0.005 and 625 respectively.

The quality of the linear models and the piecewise-linear model has been assessed using the same procedure as the one explained for X-HALE, obtaining successful results. To showcase the performance of the reduced order piecewise-linear model, a sample test case is shown in Figure 17. The reduced order piecewise-lienar model has 30 states. Time responses of UM/NAST and of a reduced order linear model obtained with balanced truncation are also plotted. The individual linear model is chosen to be the one corresponding to a representative cruise flight condition. The results show that the reduced order piecewise-linear is superior with respect standard balanced truncation of a single linear model.

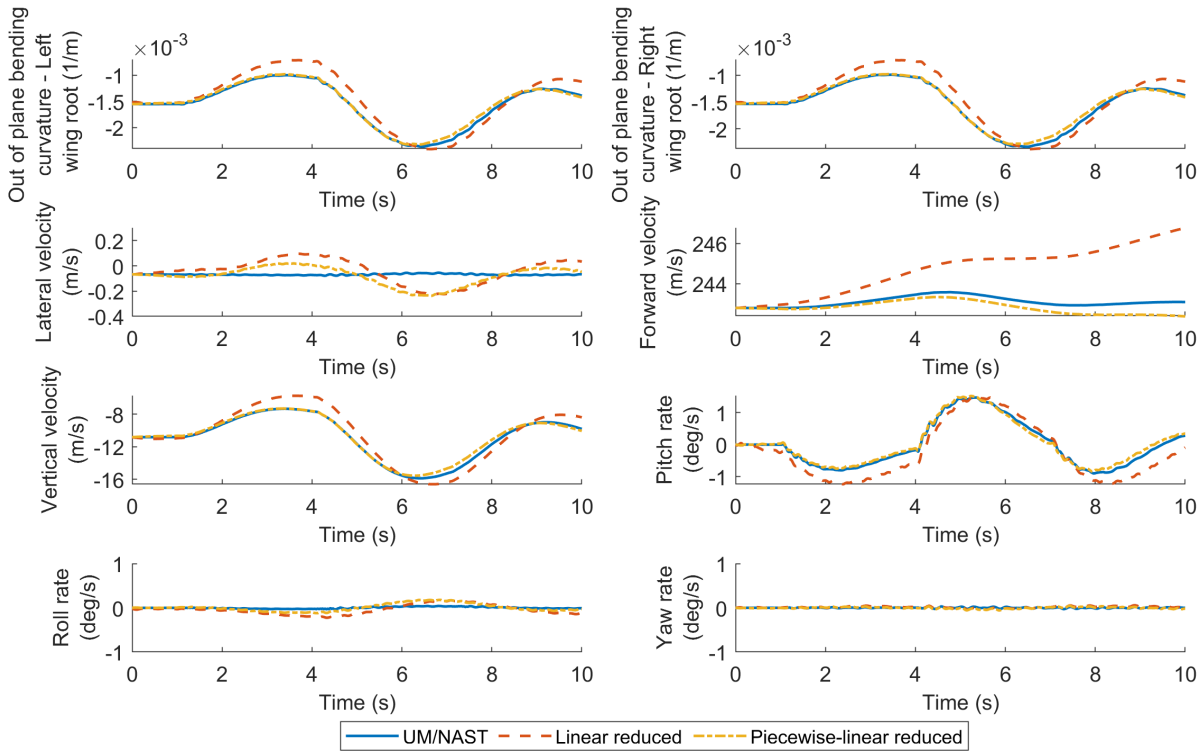

Figure 17: Time response to a doublet elevator maneuver of 0.5 deg amplitude applied to the XRF1 model initially flying trimmed at a representative cruise flight condition. Solid blue line: UM/NAST model (1013 states). Dashed red line: reduced order linear model (30 states) corresponding to a representative cruise flight condition. Dashed dotted yellow line: reduced order piecewise-linear model with distance-based interpolation weights (30 states).

6 CONCLUSIONS

The development of a model order reduction technique for very flexible aircraft has been described in this paper. Towards this end, a piecewise-linear surrogate model based on the interpolation of linear models is derived from the original nonlinear model. Two interpolation schemes have been proposed, namely one based on the definition of physical-relevant metrics to measure distance, and other more general approach that exploits neural networks. Then, the dynamics of the piecewise-linear model are projected onto a reduced order basis obtained by balanced truncation of a linearized model. The projection basis is switched periodically, obtaining in the end a hybrid system. The output of the system is continuous even when transitioning between the different bases.

Numerical examples that illustrate the application of the technique are provided. Two models have been reduced: the very flexible aircraft X-HALE, and the flexible aircraft XRF1. Both models are developed in UM/NAST. The quality of the linearizations in UM/NAST, has been assessed. Nonlinear coupling effects between longitudinal inputs/lateral outputs, and between lateral inputs/longitudinal outputs have been observed. These terms are not captured by the piecewise-linear model, but their impact in the overall dynamics of the system is small.

Regarding the piecewise-linear model, it achieves more accurate results than the individual linear models as expected. The two interpolation schemes developed have provided successful results. Although the neural network approach is more general and requires less physical insight of the system, it has some disadvantages. In particular, it is more expensive computationally and it requires careful selection of the snapshots used to train the neural network.

Finally, the reduced order piecewise-linear model outperforms classical reduced order models obtained by balanced truncation of a single linear model. The trade off between the size and accuracy of the reduced order model has been analyzed. The tests conducted show that 30-40 states are enough to capture the dynamics of the systems studied.

7 ACKNOWLEDGMENTS

The material of this paper is based upon work supported by Airbus in the frame of the Airbus-Michigan Center for Aero-Servo-Elasticity of Very Flexible Aircraft.

8 REFERENCES

[1] Hesse, H. and Palacios, R. (2014). Reduced-order aeroelastic models for dynamics of maneuvering flexible aircraft. *AIAA Journal*, 52(8), 1717–1732.

[2] Wang, Y., Song, H., Pant, K., et al. (2016). Model order reduction of aeroservoelastic model of flexible aircraft. In *Proceedings of the 57th AIAA/ASCE/AHS/ASC Structures, Structural Dynamics, and Materials Conference*. San Diego, California. AIAA 2016-1222.

[3] Zhu, J., Wang, Y., and Pant, K. (2017). Genetic algorithm-based model order reduction of aeroservoelastic systems with consistent states. *Journal of Aircraft*, 54(4), 1443–1453.

[4] de Freitas Virgilio Pereira, M., Kolmanovsky, I., Cesnik, C., et al. (2019). Model predictive control architectures for maneuver load alleviation in very flexible aircraft. In *AIAA Scitech 2019 Forum*. p. 1591.

[5] Benner, P., Gugercin, S., and Willcox, K. (2015). A survey of projection-based model reduction methods for parametric dynamical systems. *SIAM Review*, 57(4), 483–531.

[6] Baur, U., Benner, P., and Feng, L. (2014). Model order reduction for linear and nonlinear systems: A system-theoretic perspective. *Archives of Computational Methods in Engineering*, 21(4), 331–358.

[7] Sirovich, L. (1987). Turbulence and the dynamics of coherent structures, parts i, ii and iii. *Quarterly of applied mathematics*, 45(3), 561–590.

[8] Moore, B. (1981). Principal component analysis in linear systems: Controllability, observability, and model reduction. *IEEE Transactions on Automatic Control*, 26(1), 17–32.

[9] Chaturantabut, S. and Sorensen, D. (2010). Nonlinear model reduction via discrete empirical interpolation. *SIAM Journal on Scientific Computing*, 32(5), 2737–2764.

[10] Carlberg, K., Bou-Mosleh, C., and Farhat, C. (2011). Efficient non-linear model reduction via a least-squares petrov–galerkin projection and compressive tensor approximations. *International Journal for Numerical Methods in Engineering*, 86(2), 155–181.

[11] Rewienski, M. and White, J. (2003). A trajectory piecewise-linear approach to model order reduction and fast simulation of nonlinear circuits and micromachined devices. *IEEE Transactions on Computer-Aided Design of Integrated Circuits and Systems*, 22(2), 155–170.

[12] Lowe, G. and Zohdy, M. (2010). Modeling nonlinear systems using multiple piecewise linear equations. *Nonlinear Analysis: Modelling and Control*, 15, 451–458.

[13] Amsallem, D., Zahr, M. J., and Farhat, C. (2012). Nonlinear model order reduction based on local reduced-order bases. *International Journal for Numerical Methods in Engineering*, 92(10), 891–916.

[14] Amsallem, D. and Haasdonk, B. (2016). Pebl-rom: Projection-error based local reduced-order models. *Advanced Modeling and Simulation in Engineering Sciences*, 3(1), 6.

[15] Washabaugh, K., Amsallem, D., Zahr, M., et al. (2012). Nonlinear model reduction for cfd problems using local reduced order bases. In *AIAA-2012-2686, AIAA Fluid Dynamics and Co-located Conferences and Exhibit*.

[16] Gosea, I. V., Petreczky, M., Antoulas, A. C., et al. (2018). Balanced truncation for linear switched systems. *Advances in Computational Mathematics*, 44(6), 1845–1886.

[17] Gao, H., Lam, J., and Wang, C. (2006). Model simplification for switched hybrid systems. *Systems & Control Letters*, 55(12), 1015 – 1021. ISSN 0167-6911. doi: https://doi.org/10.1016/j.sysconle.2006.06.014.

[18] Zhang, L., Boukas, E.-K., and Shi, P. (2009). μ-dependent model reduction for uncertain discrete-time switched linear systems with average dwell time. *International Journal of Control*, 82(2), 378–388. doi:10.1080/00207170802126856.

[19] Aurenhammer, F., Klein, R., and Lee, D. (2013). *Voronoi Diagrams and Delaunay Triangulations*. World Scientific.

[20] Brown, E. (2003). *Integrated Strain Actuation in Aircraft with Highly Flexible Composite Wings*. Ph.D. thesis, Massachusetts Institute of Technology.

[21] Shearer, C. (2006). *Coupled Nonlinear Flight Dynamics, Aeroelasticity, and Control of Very Flexible Aircraft*. Ph.D. thesis, University of Michigan.

[22] Pang, Z. Y. (2018). *Modeling, Simulation and Control of Very Flexible Unmanned Aerial Vehicle*. Ph.D. thesis, University of Michigan.

[23] Cesnik, C., Senatore, P., Su, W., et al. (2010). X-hale: A very flexible uav for nonlinear aeroelastic tests. In *51st AIAA/ASME/ASCE/AHS/ASC Structures, Structural Dynamics, and Materials Conference, Structures, Structural Dynamics, and Materials and Co-located Conferences*.

COPYRIGHT STATEMENT